# Continuum Approaches for Describing Solid-Gas and Solid-Liquid Flow

P. Diamond

J. Harvey

H. Levine

P. Steinhardt

R. Westervelt

February 1992

JSR-91-310

Approved for public release; distribution unlimited.

This report was prepared as an account of work sponsored by an agency of the United States Government. Neither the United States Government nor any agency thereof, nor any of their employees, makes any warranty, express or implied, or assumes any legal liability or responsibility for the accuracy, completeness, or usefulness of any information, apparatus, product, or process disclosed, or represents that its use would not infringe privately owned rights. Reference herein to any specific commercial product, process, or service by trade name, trademark, manufacturer, or otherwise, does not necessarily constitute or imply its endorsement, recommendation, or favoring by the United States Government or any agency thereof. The views and opinions of authors expressed herein do not necessarily state or reflect those of the United States Government of any agency thereof.

JASON
The MITRE Corporation
7525 Colshire Drive
McLean, Virginia 22102-3481
(703) 883-6997

92 4 22 127

#### Form Approved REPORT DOCUMENTATION PAGE OMB No. 0704-0188 Public reporting burden for this collection of information is estimated to average. I hour per response, including the time for reviewing instructions, searching existing data sources, gathering and maintaining the data needed, and completing and reviewing the collection of information. Send comments regarding this burden estimate or any other aspect of this collection of information, including suggestions for reducing this burden, to Washington Headquarters Services, Directorate for information Operations and Reports, 1215 Jerfenson Davis Highway, Suite 1204, Arlington, VA. 22202-4302, and to the Office of Management and Budget, Paperwork Reduction Project (0704-0188), Washington, DC 20503. 1. AGENCY USE ONLY (Leave blank) 2. REPORT DATE 3. REPORT TYPE AND DATES COVERED February 11, 1992 4. TITLE AND SUBTITLE 5. FUNDING NUMBERS Continuum Approaches for Describing Solid-Gas and Solid-Liquid Flow PR - 8503Z 6. AUTHOR(S) H. Levine et al. 7. PERFORMING ORGANIZATION NAME(S) AND ADDRESS(ES) 8. PERFORMING ORGANIZATION REPORT NUMBER The MITRE Corporation JASON Program Office A10 JSR-90-310 7525 Colshire Drive McLean, VA 22102 9. SPONSORING/MONITORING AGENCY NAME(S) AND ADDRESS(ES) 10. SPONSORING / MONITORING AGENCY REPORT NUMBER Department of Energy JSR-90-310 Washington, DC 20585 11. SUPPLEMENTARY NOTES 12a. DISTRIBUTION / AVAILABILITY STATEMENT 126. DISTRIBUTION CODE Distribution unlimited; open for public release. 13. ABSTRACT (Maximum 200 words) Two-phase continuum models have been used to describe the multiphase flow properties of solid-gas and solid-liquid mixtures. The approach is limited in that it requires many fitting functions and parameters to be determined empirically, and it does not provide natural explanations for some of the qualitative behavior of solid-fluid flow. In this report, we explore a more recent single-phase continuum model proposed by Jenkins and Savage (1982) to describe granular flow. Jenkins and McTique (1989) have proposed a modified model to describe the flow of dense suspensions, and, hence, many of our results can be straight-forwardly extended to this flow regime as well. The solid-fluid mixture is treated as a homogeneous, compressible fluid in which the particle fluctuations about the mean flow are described in terms of an effective temperature. The particle collisions are treated as inelastic. After an introduction in which we briefly comment on the present status of the field, we describe the details of the single-phase continuum model and analyze the microscopic and macroscopic flow conditions required for the approach to be valid. We then derive numerous qualitative predictions which can be empirically verified in small-scale experiments: The flow profiles are computed for simple boundary conditions, plane Couette flow and channel flow. Segregation effects when there are two (or more) particle sizes are considered. The acoustic dispersion relation is derived and shown to predict that granular flow is supersonic. We point out that the analysis of flow instabilities is complicated by the finite compressibility of the solid-fluid mixture. For example, the large-compressibility leads to interchange (Rayleigh-Taylor instabilities) in addition to the usual angular momentum interchange in standard (cylindrical) Couette flow. We conclude by describing some of the advantages and limitations of experimental techniques that might be used to test predictions for solid-fluid flow. 14. SUBJECT TERMS 15. NUMBER OF PAGES

single-phase continuum model, acoustic modes, solid-gas, solid-liquid flows, granular flow

17. SECURITY CLASSIFICATION OF THIS PAGE

UNCLASSIFIED

UNCLASSIFIED

UNCLASSIFIED

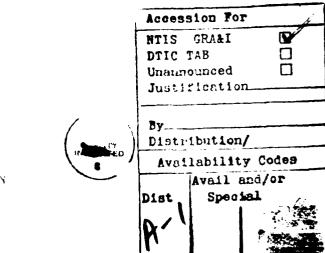
UNCLASSIFIED

SAR

#### Abstract

Two-phase continuum models have been used to describe the multiphase flow properties of solid-gas and solid-liquid mixtures. The approach is limited in that it requires many fitting functions and parameters to be determined empirically, and it does not provide natural explanations for some of the qualitative behavior of solid-fluid flow. In this report, we explore a more recent single-phase continuum model proposed by Jenkins and Savage (1982) to describe granular flow. Jenkins and McTigue (1989) have proposed a modified model to describe the flow of dense suspensions, and, hence, many of our results can be straightforwardly extended to this flow regime as well. The solid-fluid mixture is treated as a homogeneous, compressible fluid in which the particle fluctuations about the mean flow are described in terms of an effective temperature. The particle collisions are treated as inelastic. After an introduction in which we briefly comment on the present status of the field, we describe the details of the singlephase continuum model and analyze the microscopic and macroscopic flow conditions required for the approach to be valid. We then derive numerous qualitative predictions which can be empirically verified in small-scale experiments: The flow profiles are computed for simple boundary conditions, plane Couette flow and channel flow. Segregation effects when there are two (or more) particle sizes are considered. The acoustic dispersion relation is derived and shown to predict that granular flow is supersonic. We point out that the analysis of flow instabilities is complicated by the finite compressibility of the solid-fluid mixture. For example, the large compressibility leads to interchange (Rayleigh-Taylor instabilities) in addition to the usual angular momentum interchange in standard (cylindrical) Couette flow.

We conclude by describing some of the advantages and limitations of experimental techniques that might be used to test predictions for solid-fluid flow.



iii/18

# **Contents**

1	INTRODUCTION	1
2	SINGLE-PHASE CONTINUUM MODEL OF SOLID-FLUII FLOW	9
3	LESSONS FROM SIMPLE EQUILIBRIUM FLOWS	15
4	EXTENSIONS	21
5	ACOUSTIC MODES	27
6	INSTABILITIES IN GRANULAR FLOW	33
7	CONCLUSIONS	37
A	IMAGING SOLID-GAS AND SOLID-LIQUID FLOWS	39
	A.1 Non-Invasive Techniques	40
	A.2 Invasive Techniques	43

# 1 INTRODUCTION

The flow properties of solid-liquid and solid-gas mixtures are important for many problems in science and technology, including the properties of molten lavas laden with rock crystals, the dynamics of avalanches and rock slides, the flow of red blood cells through blood, the motion of sand, the processing of paper, and the transportation of petroleum and coal. These multiphase mixtures include dilute suspensions, densely packed slurries, and aerated/fluidized beds. The flow regimes can be homogeneous or heterogeneous, laminar or turbulent.

At the present time, only rudimentary progress has been made in developing a theory or an experimental database for solid-liquid and solid-gas flow even under ideal conditions, e.g., laminar flow of a monodisperse, inert, spherical particles through a cylindrical pipe. Even if progress were to be made, the problems of greatest commercial interest — coal slurry transportation and fluidization of coal beds — involve extraordinarily complex conditions far from this ideal limit. For example, a coal slurry typically entails the flow of turbulent water with 25-50% concentration density of particles with complex, chemical interparticle-forces and with a broad distribution of particle sizes and shapes. In this sense, the realistic solid-liquid or solid-gas transport problem is much less amenable to analysis than, say, the liquid-gas or liquid-liquid multiphase flow problem where both component phases can be simply described even for realistic flow conditions.

In developing an effective program of research on solid transport, therefore, a key issue is the relative reliance on research obtained from ideal systems versus efforts to improve empirical tools for realistic systems. Clearly, empirical methods will remain the necessary and key approach in engineering design, so that the design of new diagnostic tools has a high priority. For example, the ultra-sensitive capacitance and fiber-optic probes for measuring

local, time-dependent particle concentrations and velocities, which is being developed by M. Louge and E. Giannelis (Cornell), appears to be a technique that might be adapted to working conditions as well as test beds. Research on ideal systems contributes insofar as it can provide guidance in developing and refining empirical methods. For example, qualitative issues such as the distinctions between flow regimes, the scaling with pipe size, the effects of polydispersity, and the role of particle-wall interactions might be usefully addressed.

The potential contribution of research on ideal systems depends largely on the flow regime of solid transport, which can be characterized by the particle Reynolds number,  $Re|_{p}$ :

$$Re|_{p} = \frac{\rho_{o}\dot{\gamma}\sigma^{2}}{\mu_{o}},\tag{1-1}$$

where  $\rho_o$  is the density,  $\mu_o$  is the viscosity, and the relevant velocity is taken to be the local shear rate,  $\dot{\gamma}$ , times the particles size,  $\sigma$ . The cases in which research on ideal systems might best contribute are where  $Re|_p$  is either less than one or very high.

If  $Re|_p$  is less than one, the interparticle dynamics is dominated by viscous hydrodynamic forces. The particle interactions can be reasonably treated by simple kinetic theory. Hence, this regime is the one most reasonably modelled by ideal systems, as has been emphasized by Leighton and Acrivos<sup>2</sup>, and by Brady<sup>3</sup> and coworkers in their studies of dense suspensions. The condition,  $Re|_p < 1$ , applies, for example, with slurries consisting of particle sizes in the range  $a \approx 50 \mu m$  flowing in a six-inch diameter pipe at 5 ft/sec, in which case  $Re|_p \approx 3 \times 10^{-2}$ . Even though  $Re|_p$  may be small, the Reynolds number based on the macroscopic flow can be large. Hence, one may be able to model quite complex flows.

For very high particle Reynolds number, we have a different regime studied first by Bagnold.<sup>4</sup> In this limit, the momentum transfer and energy flow

are both dominated by inelastic collisions between the particles, and the suspending fluid plays a secondary role. This regime, termed "granular" flow, is relevant for such geological processes as avalanches and sand-dune formation, in addition to its relevance for solid transport e.g., circulating fluidized beds. Simple kinetic theories of particle interactions may be sufficient to explain many phenomena in this regime.

For intermediate ranges of particle Reynolds number, progress is much harder to envisage since particle collisions and hydrodynamic forces compete. We know of no good theoretical approach in this regime, nor any experimental studies to be recommended. We believe that attention should instead be focussed on the more tractable cases described above.

In addition to lying within one of the potentially tractable regimes,  $Re|_p < 1$  or  $Re|_p \gg 1$ , effective studies of ideal systems should conform to several other guidelines.

- 1. Particle properties should be kept simple. Effects such as chemical/surface interactions, electrostatic forces, van der Waals interactions, etc., should be scrupulously ignored until a fundamental understanding of simple particles is obtained. Fortunately, experimentalists appear to be able to design systems for which this abstraction is close to reality. Acrivos and various collaborators have studied the slow flow of suspensions of spheres.<sup>2</sup> Sayed and Savage<sup>5</sup> have focussed on granular flow under well-controlled conditions. In particular, they have extensively studied the validity of continuum models of granular flow and have recently produced some striking results concerning possible segregation during flow with polydisperse particles in both regimes.
- 2. Hydrodynamic properties should be tested in addition to rheological properties. Previous studies of granular flow or the flow of suspensions have emphasized rheological properties, such as effective viscosity and shear

stress. In order to discriminate among theoretical models, it is important to examine the predictions of these models for more complex hydrodynamic phenomena. For example, in the theoretical approach we will discuss in this paper, instabilities such as Taylor vortex formation for flow between rotating cylinders, shock waves in grain flow past blunt bodies, and the propagation of sound during shear flow could be critical tests of theory. These approaches probably necessitate advances in the ability to measure concentration profiles and correlation functions.

In this regard, we find the new experimental efforts to measure particle density and velocity profiles in solid-liquid flows using refraction-indexmatched glass or silica-gel particles and transparent pipelines to be especially promising, this includes both approaches using laser velocimetry (Kadambi, Case Western Reserve) and laser tagging of particles of fluid with photochemically sensitive agents (Falco, Michigan State). The recent use of x-rays to study pattern formation in granular flow (Baxter and Behringer, Duke) appears to be a major breakthrough as well. These methods should provide an important, new database for studies of monodisperse and polydisperse systems and should be continued.

3. Large-scale computation should be limited to tests of microscopic properties of multiphase flow. Several excellent papers utilizing molecular dynamics to study multiphase flow have appeared recently. This work consists of directly modeling the interparticle forces either due to hydrodynamics (Brady³, Caltech) or to collisions (Walton⁶, LLNL). Then the equations of motion can be integrated for a small (50-200) number of particles with boundary conditions imposed to mimic a particular flow, such as uniform shear. This work appears to be well-considered, and is directly coupled to the computational physics community so as to take advantage of advances in simulation capability (e.g., connec-

tion machine architecture, cellular automata, etc.) as they become available. These computer simulations can be used to evaluate the rheological properties and, hence, be validated by the aforementioned experiments. The methods can also be used to examine microscopic phenomena, such as the resuspension effect reported by Acrivos, et al.<sup>2</sup> It is clear, though, that this methodology will always be limited to small volumes and any large-scale flow is inherently untreatable. For that type of problem, a less rigorous approach, such as a continuum model, can be very useful.

4. For less rigorous approaches, such as continuum models, emphasis should be on qualitative, rather than quantitative predictions. In some studies, large-scale computations and elaborate experimental tests of models have proceeded before the basic assumptions of the model have been validated. For example, a leading theoretical approach for describing solid-fluid flow is the two-phase continuum model (R. Jackson, Princeton; D. Gidaspow, IIT). This approach is limited at the outset since it depends on many unknown functions that must be fit to experiments before any new predictions can be made. More importantly, the simplest versions fail to properly predict some gross, qualitative features, such as the sensitivity of the bubble formation to the viscosity of the suspending fluid. The response has been to appeal to additional effects requiring the fitting of new unknown functions. In this way, the model has evolved to be more and more complicated with less and less real predictive power.

In spite of these drawbacks, significant resources have been focussed towards experimental measurements of the fitting functions and large-scale computations of macroscopic flow conditions. In one case, a project to develop high-quality test stations to study flow properties in circulating fluidized beds (T. Knolton, IGT) has been slaved, in part, to measure parameters for large-scale computer simulations of

one particular two-phase continuum model (D. Gidaspow, IIT). While we endorse the construction of the test station and the development of an empirical database, we strongly recommend decoupling the experimental and theoretical programs. In fact, we would discourage the large-scale simulations of continuum models altogether until qualitative issues have been more adequately addressed. One needs first to critically evaluate whether the entire approach is valid, perhaps looking for further qualitative tests of the theory.

As an example of the approach we are recommending, we present below a discussion of a promising, alternative continuum model for solid-liquid and solid-gas flow that has been developed by Jenkins and Savage, McTigue and Jenkins, and Haff<sup>10</sup>. The model treats the solid-fluid mixture as a single-phase, compressible fluid in which an effective temperature is introduced to describe the particle fluctuations. This model attracted our attention because, compared to the two-phase models, it appears to be a simpler, more intuitive approach with fewer unknown parameters. We develop the theory to the point where we can suggest simple, qualitative tests to determine whether the basic assumptions are workable. Only after such validation would we suggest detailed computations of flow properties, such as viscosity dependence on concentration or particle properties. Also, we would suggest a cautious apprach toward immediate extensions of the theory to the highly turbulent granular regime, as has been suggested by M. Louge and J. Jenkins, until the model has proved useful in the simpler flow regimes.

The plan of the report is as follows. In Section 2, we outline the continuum theory of Jenkins and coworkers. In Section 3, we apply the model to various simple equilibrium flow situations. We derive an important consistency requirement for equilibrium which amounts microscopically to the balance between viscous heating by the shear and collisional dissipation. We also point out some possible ways to extend the current theory. For example,

we introduce convective-diffusion terms to describe the observed segregation in polydisperse flows. In Section 4, we address the consequences of having the solid-fluid system described by a compressible flow. We show that granular flows support sound waves which are typically much slower than the local flow rate. Hence, many systems will be in the supersonic regime so that one may expect to observe shock waves of concentration in granular flow. (Perhaps the theory can be extended to explain the concentration shock waves that have been observed by Baxter and Behringer under conditions different from simple shear flow.) We also discuss the consequences of fluid compressibility for the instabilities, such as in Couette flow. As an Appendix, we discuss existing and potential experimental imaging techniques for solid-fluid flow, the critical component for testing theoretical predictions.

# 2 SINGLE-PHASE CONTINUUM MODEL OF SOLID-FLUID FLOW

In this section we describe the single-phase continuum model developed by Jenkins and Savage<sup>8</sup> to describe granular flow, a regime which includes fluidized beds and rapidly flowing sand. We will also briefly discuss more recent work<sup>9</sup> by Jenkins and McTigue using the same framework to describe dense suspensions.

The model is designed to describe a moderately concentrated granular fluid of monodisperse, chemically inert, spherical particles. In the next section, we will discuss how the theory might be modified to describe a fluid with a distribution of particle sizes. Moderate concentration means that the particle diameter,  $\sigma$ , is larger than the average spacing between grain surfaces, h, but the system is not so densely packed that particles become jammed together, thus preventions velocity fluctuations. To estimate the relation between the fractional volume concentration,  $\phi$ , and  $h/\sigma$ , note that the fluid would become dense-random-packed if each particle were suddenly increased in diameter by h; hence,

$$\frac{h}{\sigma} \left( \frac{\phi_{DRP}}{\phi} \right)^{1/3} - 1, \tag{2-1}$$

where  $\phi_{DRP} \approx .62$  is the fractional volume for dense-random-packed spheres. By moderate concentration, then, we refer to  $\phi$  between .2 and .5 or  $h\sigma$  between .1 and .5.

The model approach is to treat the granular system as a single-phase, compressible, continuum fluid. For deriving the constitutive relations, we need to introduce the concept of a "temperature" related to the local velocity fluctuations about the mean flow. If  $v_T$  is the average fluctuating velocity, the fluctuation temperature, T, is defined to be  $\sim v_T^2$ . The average time between collisions is  $\tau = \frac{h}{v_T}$ .

The model is similar to the model for a classical, dense gas, but there are two important distinguishing features. First, we expect the collision between granular particles to be inelastic. We define a typical fractional energy lost per collision to be 1 - e; in practice e ranges from nearly 1 (elastic) to much smaller values for non-spherical shapes. In systems of interest, e is probably in the range .7-.9. Second, the source of "heat" in the granular flow problem is flow inhomogeneities or shear; there is no direct analogue of heat sinks or sources that can be introduced at the boundary.

The continuum equations follow straightforwardly from the continuity condition and conservation of momentum and energy:

$$\frac{d\rho}{dt} = -\rho \vec{\nabla} \cdot \vec{v} \tag{2-2}$$

$$\rho \frac{d\vec{v}}{dt} = -\vec{\nabla}p + \vec{\nabla} \cdot \vec{t} \tag{2-3}$$

$$\frac{d\rho}{dt} = -\rho \vec{\nabla} \cdot \vec{v} \qquad (2-2)$$

$$\rho \frac{d\vec{v}}{dt} = -\vec{\nabla}p + \vec{\nabla} \cdot \vec{t} \qquad (2-3)$$

$$\frac{3}{2}\rho \frac{dT}{dt} = \vec{\nabla} \cdot (k\vec{\nabla}T) - p\vec{\nabla} \cdot \vec{v} + \vec{t} \cdot \vec{\nabla}v - \Gamma \qquad (2-4)$$

where p is the pressure, k is the thermal diffusivity, and  $\Gamma$  is the energy loss rate per unit volume. The stress tensor,  $t_{ij} \equiv \mu(d_{ij} + c_1 \delta_{ij} \vec{\nabla} \cdot \vec{v})$ , can be expressed in terms of the symmetric strain tensor, d, the viscosity,  $\mu$ , and a constant of order one,  $c_1$ . Note that we intend the time-derivatives to be substantive; e.g., the left-hand-side of Equation (2-2) includes a spatial gradient of the density,  $\rho$ .

The granular flow regime is defined as the limit in which the energy and momentum transport are dominated by particle collisions. Hence, the transport coefficients,  $\mu$ , k, and  $\Gamma$ , and the pressure can be straightforwardly estimated in terms of the average fluctuation velocity, vT, the particle mass m, the particle diameter,  $\sigma$ , and the mean separation, h. It is sometimes useful to express these estimates in terms of the fluctuation temperature, T, and the particle mass density,  $\rho \approx m/\sigma^3$ .

1. The viscosity  $\mu$  is proportional to the ratio of cross-stream momentum transport to the shear rate,  $\dot{\gamma}$ :

$$\begin{array}{rcl} \text{Momentum} &\cong & \frac{\text{Momentum}}{\text{Area-Time}} \\ &\cong & (m\Delta v)\sigma^{-2}\tau^{-1} \\ &= & \left(\frac{m\sigma\dot{\gamma}}{\sigma^3}\right)\sigma\frac{v_T}{h} \\ &= & \frac{\sigma^2}{h}\rho v_T\dot{\gamma}. \end{array}$$

Hence, an estimate for the viscosity is  $\mu = \mu_o \rho T^{\frac{1}{2}}$ , where  $\mu_o \propto \sigma^2/h$ .

2. Thermal Diffusivity is proportional to the ratio of the energy flux to the thermal gradient:

Energy flux 
$$\approx \left(\frac{m\Delta T}{\sigma^2 \tau}\right)$$
  
=  $\rho \frac{\sigma^2}{h} v_T \frac{dT}{dz}$ ,

Hence, the thermal diffusivity is  $\kappa = \kappa_o \rho T^{\frac{1}{2}}$  where  $\kappa_o \propto \sigma^2/h$ .

3. Energy loss rate per unit volume:

$$\Gamma \approx (1 - e) \frac{mT}{\sigma^3 \tau}$$
$$= (1 - e) \rho \frac{T^{\frac{3}{2}}}{h}$$

Therefore,  $\Gamma = \Gamma_o \rho T^{\frac{3}{2}}$  where  $\Gamma_o \propto (1 - e)/h$ .

4. Pressure is the force per unit area produced by the collisions:

Pressure 
$$\approx \frac{(m\Delta v)}{\sigma^2 \tau}$$
  
 $\approx \rho v_T \sigma \frac{v_T}{h}$ .

So, the equation of state is similar to that of an ideal gas,  $p = p_o \rho T$ , where  $p_o \propto \sigma/h$ .

This model is clearly simplistic, even for a monodisperse distribution of spherical particles. Specifically, it does not take account of rotation and sliding friction between particles. Consequently, the model is applicable, at best, over a restricted range of concentrations and velocities. Sliding friction, for instance, becomes especially important at low velocities and high concentrations. Real flowing sand forms sandpiles (or sand dunes) stabilized by sliding friction as the velocity becomes small, yet a continuum fluid model of the type described would predict a "sand puddle" instead! Similarly, Behringer<sup>11</sup> has noted some distinctions between flow of smooth versus irregular particle in his studies of 2D flow down a hopper. The concept of local sliding is connected to the local orientation of the grains which has not been included in theories to date. We can envisage a theory which couples the translational motion to the local rotation, which is then hindered by friction. For now, we will argue that the present model may be applicable for rather homogeneous flows at intermediate concentrations and high velocities. If the model is proved successful in such regimes, it will justify working to enhance the model to include rotation and sliding friction effects.

Recently, Jenkins and McTigue<sup>9</sup> have suggested modifying this framework to describe flows in dense suspensions. In this regime, particle fluctuations may play a role similar to that in granular flows. The key difference is that the interaction between forces is effected through interstitial viscous fluid, via lubrication forces, rather than by partial collisions. Hence the dissipation due to inelastic collisions between particles (proportional to  $1 - \epsilon$ ) is no longer important. At high concentrations, these forces are dominated by lubrication forces, so  $\Gamma$  scales as  $\nu T/\sigma h$ , where  $\mu$  is the interstitial fluid viscosity.

In the viscous hydrodynamic regime, the momentum flux scales as  $\nu T^{\frac{1}{2}}/\sigma$ , (compared with  $\rho T$  for the granular regime). Hence, we must replace

$$\rho \to \frac{\mu}{\sigma\sqrt{T}},\tag{2-5}$$

representing a change from inertial forces to viscous forces. By replacing  $\rho$  in each of the expressions above, we obtain the Jenkins and McTigue model for dense suspensions.

One fine point is that the non-Newtonian character of the flow (as evidence by a non-vanishing contribution to the normal stress) is small consistent with the fact that it is strictly absent for spherical particles in the hydrodynamic limit. In real dense suspensions, though, the normal stress contribution may not be so negligible even in the hydrodynamics regime, as has been stressed by Leighton and Acrivos.<sup>2</sup> This is due to the particle shape and asperity (surface roughness) which can effectively lock particles together during a collision and transfer momentum perpendicular to the shearing direction. It would be useful to extend this model (and the dynamical computer simulations of Brady<sup>3</sup>) to include this effect.

# 3 LESSONS FROM SIMPLE EQUILIBRIUM FLOWS

In this section, we apply the Jenkins and Savage model to various equilibrium flow problems. Our goals are to establish the conditions under which the model might be valid, and to develop physical intuition about model predictions for simple flow conditions.

EXAMPLE 1: Let us suppose that we can fix the entire mean velocity field to be oriented along the x-direction with uniform gradient in the z-direction:

$$\vec{v} = v_o \left( 1 + \frac{z}{L} \right) \hat{x}; \tag{3-1}$$

or, equivalently there is a constant shear rate,  $\dot{\gamma} = v_o/L$ , where L is the size of the system. In equilibrium, the energy balance equation, Equation (2-4), becomes:

$$0 = \vec{\nabla} \cdot (\kappa \vec{\nabla} T) + \vec{t} \cdot \vec{\nabla} v - \Gamma \tag{3-2}$$

$$= \frac{\partial}{\partial z} \left( \kappa_0 \rho T^{\frac{1}{2}} \frac{\partial}{\partial z} \right) + \mu_o \rho T^{\frac{1}{2}} \left( \frac{v_o}{L} \right)^2 - \Gamma_o \rho T^{\frac{3}{2}}. \tag{3-3}$$

The solution of this equation (also consistent with the continuity and momentum balance equations) is:

$$\frac{dT}{dz} = 0 \quad T = \text{constant} \tag{3-4}$$

$$v_T^2 = 2\frac{\mu_o}{\Gamma_o} \left(\frac{v_o}{L}\right)^2 \tag{3-5}$$

$$\approx \left(\frac{\sigma}{L}\right)^2 \frac{v_o^2}{1-e}.\tag{3-6}$$

The solution means that the assume flow profile corresponds to thermal equilibrium for fluctuations in the granular regime. The temperature results from shear: the greater the shear rate  $\dot{\gamma}$ , the higher the fluctuation temperature, T. The single-phase continuum approach, if it is valid in any regime, should be able to predict properties of flows near this limit.

One should also bear in mind that any continuum model assumes that the particle diameter  $\sigma$  is small compared to the system size L. Hence, from Equation (3-6), we discover that the mean fluctuation velocity  $v_T$  is much less than mean flow velocity  $v_o$ . We shall find this result to be of critical importance in the sound speed analysis presented in the next section.

The momentum balance equation, Equation (2-3), for the  $\hat{z}$  direction yields the requirement of constant pressure, which, combined with the constant temperature derived above, yields a constant density profile. Given the result for  $v_T$ , this predicts that the pressure (normal stress) and the shear stress  $\simeq \mu \frac{\partial v}{\partial z}$  are both proportional to  $(\dot{\gamma})^2$ . This prediction may be regarded as a critical qualitative test of whether a given granular flow is in the range of velocity and concentration parameters appropriate for description by the single-phase continuum model.

As it turns out, this proportionality to the square of shear rate agrees over the range of moderate concentrations and high velocities (perhaps appropriate for fluidized beds) in experiments by Bagnold<sup>4</sup> and Sayed and Savage<sup>5</sup>, as well as computer simulations of Walton *et al.*.<sup>6</sup> (where sliding friction is neglected). Hence, even though we argued previously that the model fails at low velocities and very high concentrations (e.g., sandpiles), there seems to be a physically interesting regime of concentrations and velocities where the single-phase continuum model may be valid.

EXAMPLE 2: We now give a more precise treatment of the shear flow case. We consider flow between two parallel plates at  $z = \pm H$  at which there are imposed velocities  $v(z = \pm H) = \pm U$ . We will assume that the granular fluid obeys a non-slip boundary condition – this is almost certainly not precisely true but our interest in qualitative findings allows us this simplification.

Unlike example 1 where we imagined fixing  $\frac{\partial v}{\partial z}$  to be constant throughout

the bulk, here v is fixed only on the boundary; the interior behavior must be obtained by solving the equations of motion. By symmetry, the physical variables v, T, and p should depend on z only, and this dependence should be determined by solving the continuity, momentum balance and energy balance equations, Equations (2-2) through (2-4). The continuity equation, Equation (2-2), is satisfied trivially since v is divergenceless. There remains the momentum balance (along two independent directions) and energy balance equations:

$$0 = \frac{\partial}{\partial z} \left( \mu_o \rho T^{\frac{1}{2}} \frac{\partial v}{\partial z} \right) \tag{3-7}$$

$$0 = \frac{\partial}{\partial z}(\rho T) \tag{3-8}$$

$$0 = \kappa_o \frac{\partial}{\partial z} \left( \rho T^{\frac{1}{2}} \frac{\partial T}{\partial z} \right) - \rho \Gamma_o T^{\frac{3}{2}} + \mu_o \rho T^{\frac{1}{2}} \left( \frac{\partial v}{\partial z} \right)^2. \tag{3-9}$$

These equations imply  $T = \frac{\rho_o}{\rho}$  with  $\rho_o$  a constant of integration which must be fixed by the total density, and  $\frac{\partial v}{\partial z} = AT^{\frac{1}{2}}$  where A is a second constant of integration.

Substituting into the energy balance equation, we find

$$\kappa_o \frac{\partial}{\partial z} \left( \rho_o T^{-\frac{1}{2}} \frac{\partial T}{\partial z} \right) = 2 \frac{\partial^2}{\partial z^2} (\kappa_o \rho_o T^{\frac{1}{2}}) = \lambda \kappa_o \rho_o T^{\frac{1}{2}}, \tag{3-10}$$

where

$$\lambda = \frac{\Gamma_o}{\kappa_o} - A^2 \frac{\mu_o}{\kappa o}.\tag{3-11}$$

This equation is directly solvable for the temperature field and implies that the temperature varies, with spatial rate  $\sqrt{|\lambda|}$ . But  $\lambda$  is not yet known, since it depends explicitly on the constant of integration A. To fix  $\lambda$ , we need to specify a boundary condition on  $\partial T/\partial z$  corresponding to the energy flux from the walls. If  $\partial T/\partial z = 0$ , we then must have

$$A^2 = \frac{\Gamma_o}{\mu_o}$$

corresponding to precise balance between energy loss and viscous "heating" due to the shear flow. More generally, however, the flux will not be zero and in typical computer experiments appears to be positive (see Campbell<sup>(12)</sup>). This means that a solution to the temperature equation has the form

$$T^{\frac{1}{2}} = E \cosh \lambda z \tag{3-12}$$

with E determined via the equation

$$\left. \frac{\partial T}{\partial z} \right|_{z=H} = 2E^2 \cosh \lambda H \sinh \lambda H$$

once  $\lambda$  is known. We then use  $\frac{\partial v}{\partial z} = AT^{\frac{1}{2}}$  to find the velocity field

$$v(z) = \frac{AE \sinh \lambda z}{\lambda}. (3-13)$$

Imposing  $v(\pm H) = \pm U$  gives the relationship

$$U = \frac{AE}{\lambda} \sinh \lambda H \tag{3-14}$$

determining A in terms of  $\lambda$ . This is then combined with Equation (3-11) to find an equation for  $\lambda$ , so the system closes consistently.

The preceding analysis is important since there appears to be some confusion in the literature regarding exactly how many boundary conditions one should impose. Our approach seems to agree with that of Johnson and Jackson<sup>13</sup> but disagrees with that of Hanes, Jenkins and Richman<sup>14</sup>. In the latter paper, there is an additional restriction placed on the normal stress, as opposed to considering just energy and tangential stress (which we have approximated as no slip). This leads to a condition on the depth of the layer H which is not physical. This is recognized by the authors who relax the density equation near the boundary. Our perspective is that if the idea of bulk flow equation makes sense, one must be able to coarse grain over all boundary effects and recover two boundary conditions.

In the next section, we will discuss approximate methods for including friction in the above calculation. For the moment, we note that it is clear that for any finite  $\lambda$ , the above theory must break down if the depth H is made too large. This is simply because the temperature decreases rapidly as we leave the boundary and the density increases; at some point the density is so large as to cause the grains to interlock and prevent motion. In fact, one item which a full theory should predict is exactly this maximum depth H. We will return to this in the next section.

EXAMPLE 3: Example 2 can be modified to describe channel flow between two stationary parallel plates. We choose the boundary conditions  $v(z=\pm H)\approx 0$ , assuming that the velocity is nearly zero at the particle-plate interface. A constant force F is then imposed along the flow direction (x-axis). The equation so motion are the same as in Example 2, except that F is added to the right-hand-side of the momentum balance equation for the x-direction. Consequently, we still have  $T=\frac{\rho_o}{\rho}$  (where  $\rho_o$  is an integration constant), but now

$$\mu_o \rho T^{\frac{1}{2}} \frac{\partial v}{\partial z} = A - Fz.$$

Because the channel flow problem is symmetrical about z=0, there is the constraint that  $\left|\frac{\partial v}{\partial z}\right|_{z=0}=0$ , or A=0. Hence,

$$\frac{\partial v}{\partial z} = \left(\frac{F}{\mu_0 \rho_0}\right) T^{\frac{1}{2}} z. \tag{3-15}$$

If T were constant, the solution would describe the parabolic velocity profile characteristic of channel flow. Substituting this expression for the velocity gradient into the energy balance equation, Equation (2-4), we obtain the same equation for the temperature profile as before, Equation (3-10), except that  $\lambda$  is replaced by:

$$\lambda = \left[ \frac{\Gamma_o}{\kappa_o} - \left( \frac{F^2}{\kappa_o \mu_o \rho_o^2} \right) z^2 \right]. \tag{3-16}$$

To describe the solution to the temperature profile equation it is useful to recast the equation in the form:

$$\frac{d^2\Theta}{dz^2} + \left[\alpha z^2 - \beta\right]\Theta = 0, \qquad (3-17)$$

where  $\Theta=T^{\frac{1}{2}}$ ,  $\alpha=\left(\frac{F^2}{\kappa_o\mu_o\rho^2}\right)$  and  $\beta=\frac{\Gamma_o}{\kappa_o}$ . The general solution can be expressed in terms of parabolic cylinder functions. If  $D_v(x)$  is the parabolic cylinder function for real v, then the general solution to Equation (3-15) can be expressed in terms of the real and imaginary parts of  $D_{\gamma}(e^{i\pi/4}(4\alpha)^{1/4}z)$ , where  $\gamma=i\beta(4\alpha)^{-1/4}$ . Linear combinations of these functions should be taken which respect the symmetry under  $z\to -z$ .

Just as in the previous case, one needs to know the boundary condition to find the actual profile. Here, fixing  $\partial T/\partial z$  will, together with the symmetry of the temperature profile, enable a complete determination of  $\Theta$ ; unlike the shear flow, the temperature cannot be constant since  $\lambda$  is fixed by the external forcing, not by the internal dynamics. All in all, the lesson is that granular channel flow is complicated compared to the standard Poiseulle problem.

EXAMPLE 4: In this example, we return to the problem of shear flow of Example 2, but here with a gravitational field superimposed in the z direction (perpendicular to the shear planes). The momentum balance equation for the z-direction is changed to:

$$\frac{\partial}{\partial z}(\rho T) = -\rho G,\tag{3-18}$$

so pressure,  $p \propto \rho T$ , decreases upward. The equation can be satisfied by either a temperature gradient (colder upward) or a density gradient (less dense upward) or both. However, if the continuum model is to be valid, gravity must be a small perturbation compared with the fluctuation energy:  $gz \ll T$ . From the previous example, we know that  $\rho$  and T vary nearly inversely as  $g \to 0$ . Since the temperature is more effective at balancing the gravitational force in Equation (3-18) (the density variation adds a term of the form  $T\frac{\partial ln\rho}{\partial z}$ ), the solution must be that the temperature gradient will point downward.

# 4 EXTENSIONS

There are several directions in which it might be possible to extend the considerations of the previous sections. Perhaps the most crucial issue is how to include frictional forces, but experiments involving particle size segregation also may be worth examining. In this section we take a preliminary look at these two issues. In the next section, we discuss a different direction, that of acoustic waves in granular flows.

Let us start with the issue of polydispersity. In many experiments (see e.g. Savage and Lun<sup>15</sup>), there is an obvious tendency of particles to segregate with the small ones falling to the bottom. Microscopically this happens because the small particles can fall through the holes made by the dynamical motion of the large particles but not vice versa. We will try to study a simpler case, that of a few large particle moving in a continuum of small ones. We will postulate that the large particle concentration obeys a diffusion equation

$$\vec{\nabla} \cdot (D_{eff} \vec{\nabla} c) \sim \frac{dc}{dt}.$$
 (4-1)

We might suppose that the effective diffusivity, in analogy with Einstein formula, should be of order

$$D_{eff} \sim \frac{\rho kT}{6\pi\bar{\mu}R_o} \tag{4-2}$$

for particles of radius  $R_o$  in a medium with effective viscosity  $\bar{\mu}$ .

Recall, then, the case of shear flow in a gravitational field, Example 4. The viscosity is  $\rho T^{\frac{1}{2}}$ , where the temperature gradient points downward. Hence,  $D_{eff} \propto T^{\frac{1}{2}}$  and  $\nabla D_{eff}$  is in the  $-\hat{z}$  direction. From the above equation,

$$\frac{dc}{dt} - \vec{\nabla}D_{eff} \cdot \vec{\nabla}\dot{c} = D_{eff} \nabla^2 c \tag{4-3}$$

implies that  $\nabla D_{eff}$  acts as a negative convective term. The conclusion is that the large particles tend to be carried upward. In a centrifugal flow, this would be upward and inward.

This may be a possible macroscopic explanation for vertical segregation effects.<sup>5</sup> Note that this approach is consistent with the aforementioned microscopic explanation: all particles try to move in the forcing direction (downward) but the smaller particles moves more efficiently, creating a new backflow of larger particles. Of course, since we have treated the small grains as a continuum fluid which suspends the larger particles, the approximations breakdown if the larger (impurity) particles were to be replaced by impurities smaller than the grains. This break down is just as well since, in this case, the impurities should fall, not rise.

As the size and density of the impurities becomes comparable to smaller ones, one should take account of their velocity fluctuations as well. If the larger particles were to begin near the bottom of the shear flow above, they would be in a high T region, driven by both a thermal and concentration diffusivity whose values could be quite different. The situation is analogous to double diffusive convection of salt in seawater heated by the sun. (Of course, the geometry is upside-down compared to the granular flow problem in the sense that the higher temperature and concentration is at the top for the salt example but at the bottom for the shear flow problem.) By this analogy, one would expect convection of the larger particles though the formation of "fingers" containing high concentrations of large particles extending upward from the bottom shear plane. If a similar analysis is applied to the viscous hydrodynamic regime, it may provide an explanation of the fingering effects reported by Weiland, et al. 16 Here, particles of unequal weight and/or size segregate into filaments during sedimentation. Fluctuations in the particle size distribution could lead to more rapid sedimentation, larger shear and a horizontal hydrodynamic force leading to further separation.

The above discussion based on a single impurity can easily be extended to describe a finite concentration of impurities. We argued that an approximate solution to the equation of motion, Equation (3-18), for shear flow in a vertical gravitational field is  $\rho \approx \text{constant}$  and, hence,  $T \approx T_o - Gz$ , where

 $T_o$  is an integration constant. In equilibrium, Equation (3-21) predicts that

$$D_{eff}\nabla^2 c = -\nabla D_{eff} \cdot \nabla C,$$

where

$$D_{eff} \propto T^{\frac{1}{2}} \approx (T_o - gz)^{\frac{1}{2}}.$$

Hence, the model predicts an equilibrium profile of the form

$$\frac{\partial c}{\partial z} = \frac{g}{2} \ln (T_o - gz). \tag{4-4}$$

Several considerations should be taken into account before applying these qualitative conclusions to real experiments. First, in computing the diffusivity, we have used the Einstein formula which assumes viscous flow about the large particle impurities. However, we will argue in the next section that the granular flow about an obstacle is likely to be supersonic and contain shock waves. Thus, it is not clear whether the effective diffusivity decreases with increasing  $R_o$  or not, as the Einstein relation would predict. We raise this qualification because the microscopic theory would predict that impurities with larger radius rise more rapidly, whereas the argument above predicts the opposite (see Equation (3-20)). One possibility is that both predictions are correct: that diffusivity increases with particle radius if the impurity diameter is modestly greater than the grain size, but the opposite holds in the limit when the grain size is much smaller than the impurities. In this case, it should be very interesting to study experimentally the crossover from microscopic to continuum-granular behavior as a function of impurity size.

Second, we note that experiments which are reported to produce the segregation effect are vertical shaking of the granular material rather than shear. It may be that this is just a means of producing an increased temperature and higher effective diffusivity. A revealing test would be to study vertical shaking versus shear and to discover how diffusivity scales with particle size.

Third, the above estimate will break down if the temperature change due to gravity becomes comparable to the shear induced temperature:

$$gH \ge \frac{\sigma^2}{1 - e} \left(\frac{v_o}{L}\right)^2,\tag{4-5}$$

where the shear rate is  $v_O/L$ . If we use a grain size of 100  $\mu$ m in a box of size 1 cm, our estimates become invalid for velocities less than 30 m/sec or so. This emphasizes the fact that the local shear must be rather large for it to dominate gravity in the particle dynamics.

We now turn to the issue of friction. As already mentioned, we cannot have infinitely deep granular flow regimes because the temperature rapidly decreases away from the boundary. Even in the case where the temperature was constant ( $\lambda = 0$ ), including gravity will cause the density to increase with depth and limit the extent of the granular flow layer.

The simplest estimate one can make for this effect is to take an all or nothing approach to frictional forces. That is, one can drop friction completely in the granular flow regime but require that the flow be sufficiently vigorous to overcome sliding. This means that the ratio of shear stress  $\tau$  to normal stress must be greater than  $\tan \phi_{\tau}$ , where  $\phi_{\tau}$  is the angle of repose. This is the angle that a sandpile adopts as it flows (see later). Using a simple assumption of constant density, we find (Hanes and Inman<sup>17</sup>)

$$\tau = \tau_o$$

$$p = p_o - \int_H^z \rho g dz = p_o + \rho g (H - z)$$

so,

$$H - z = \left(\frac{\tau_o}{\tan \phi_r} - p_o\right) / \rho g.$$

This predicts that the layer depth for the system should increase with shear rate, since  $\tau_o$  and  $p_o$  increase. If we measure  $\tau_o$ ,  $p_o$  and the layer depth, however, we can use the above formula to find an effective value of  $\phi_\tau$  which should be independent of shear rate. Experimentally, this appears to be

roughly true, but there is a systematic increase with shear rate which is not explained by this approach.

How might one do better. First, we have not properly taken into account the fact that the density is not constant. Solving for the density involves finding the temperature profile (using the energy equation and boundary conditions) and using the equation of state. We expect, of course, for the density to increase as we go downward and this complicates the simple linear relationship given above. Since this effect undoubtedly depends on shear rate, this could explain the deviation.

Another possibility is that one must take into account friction for the granular flow itself. Roughly, as the density increases, particle contact begin to be dominated by sliding and the pressure goes up. A phenomological approach to this idea has been put forth by Johnson and Jackson<sup>(13)</sup> based on critical state soil theory, but this approach is not very compelling. Again, this will change the simple relationship between depth and the angle of repose and could explain the data.

It is worth pointing out that one must be careful in using the idea of a fixed angle of repose. As has been stressed by Nagel<sup>(18)</sup> (and is apparently well known in the sand community) there are actually two angles corresponding to static friction and dynamic friction. The larger angle  $\phi_m$  is the largest angle for a sandpile; once this angle is exceeded, the pile flows and relaxes back to the angle of repose  $\phi_r$ . In some sense, there is a range of angles  $\phi_r \leq \phi \leq \phi_m$  at which a granular fluid can coexist with a granular solid. The natural assumption that the actual equilibrium point lies at  $\phi_r$  may not be accurate. This too may offer an explanation for the observed variation in the friction angle.

There is a completely different approach to granular flow that starts with the static granular solid and attempts to model flow via plasticity equations. This appears to be the standard methodology employed for the design of grain silos, for example. We would like to point out that there is increasing evidence that this approach fails; this evidence includes instabilities of the basic assumed profiles (Schaeffer<sup>19</sup>) and the apparent lack of correlation with experimental findings (see Reference 2). So, although there is as yet no completely consistent method of including friction in the granular flow theories, we view this way of approaching the problem as more productive than the idea of starting with the solid and including motion.

## 5 ACOUSTIC MODES

Let us return to the simple constant temperature profile discussed in Section 3. As Haff<sup>10</sup> has already noted, it is likely that there will be important effects due to density variations during granular flow. This is true because the collision frequency and hence the transport depends strongly on the density. We will study this issue by focussing on the acoustic modes of the granular fluid.

Let us consider the linearized version of the fluid equation; we will assume that the acoustic mode is propagating in the  $\hat{y}$  direction, normal to the x-z shearing plane. The equations are

$$\frac{\partial \rho'}{\partial t} = \frac{-\partial}{\partial y} \rho^{(o)} u'$$

$$\rho^{(o)} \frac{\partial u'}{\partial t} = \rho^{(o)} \frac{\partial}{\partial y} \left( \frac{\rho'}{\rho^{(o)}} + \frac{T'}{T^{(o)}} \right) + \mu^{(o)} \frac{\partial^2 u'}{\partial y^2} (2 + c_1)$$

$$\frac{3}{2} \rho^{(o)} \frac{\partial T'}{\partial t} = \kappa^{(o)} \frac{\partial^2 T'}{\partial y^2} - p^{(o)} \frac{\partial u'}{\partial y} + \mu^{(o)} \left( \frac{\partial v^{(o)}}{\partial z} \right)^2$$

$$\cdot \left( \frac{\rho'}{\rho^{(o)}} + \frac{1}{2} \frac{T'}{T^{(o)}} \right) - \Gamma^{(o)} \left( \frac{\rho'}{\rho^{(o)}} + \frac{3}{2} \frac{T'}{T^{(o)}} \right).$$

Here the superscript <sup>(o)</sup> means the value in the base solution including the density and temperature dependence. For example

$$\Gamma^{(o)} = \rho^{(o)} T^{(o)3/2} \Gamma_o$$

In the last equation, we can simplify the right hand side by noting the  $\lambda=0$  equilibrium condition

$$\mu^{(o)} \left( \frac{\partial v^{(o)}}{\partial z} \right)^2 = \Gamma^{(o)}.$$

This then implies that the last two terms collapse to the simpler form

$$-\frac{\Gamma^{(o)}T'}{T^{(o)}}$$
.

To proceed, we take a time derivative of the density equation and use the momentum equation for the  $\hat{y}$  velocity u'. This yields

$$\frac{\partial^2 p'}{\partial t^2} = c_t^2 \frac{\partial^2 \rho'}{\partial y^2} + c_\rho^2 \frac{\partial^2 T'}{\partial y^2} - \frac{\mu^{(o)}}{\rho^{(o)}} (2 + c_1) \frac{\partial^3 \rho'}{\partial y^2 \partial t}$$

where the isothermal sound speed  $c_t^2 = \frac{\partial p}{\partial \rho}\Big|_T$  and  $c_\rho^2 = \frac{\partial p}{\partial T}\Big|_\rho$ . The energy equation using the above simplification has the form

$$\frac{3}{2}\rho^{(o)}\frac{\partial T'}{\partial t} = \kappa^{(o)}\frac{\partial^2 T'}{\partial y^2} + \frac{p^{(o)}}{\rho^{(o)}}\frac{\partial \rho'}{\partial t} - \frac{\Gamma^{(o)}T'}{T^{(o)}}.$$

Assume the dependence for  $\rho'$ , T' of  $e^{(iky-\omega t)}$ , we find the eigenvalue equation

$$0 = \det \begin{pmatrix} c_t^2 k^2 + \omega^2 - i\omega k^2 \nu' & c_\rho^2 k^2 \\ + \frac{i\omega c_t^2}{\frac{3}{2}\rho(\rho)\chi} & \frac{-i\omega}{\chi} + k^2 + \frac{\omega_c}{\chi} \end{pmatrix}$$

where

$$\nu' = \frac{\mu^{(o)}}{\rho^{(o)}} (2 + c_1)$$

$$\chi = \frac{k^{(o)}}{3/2\rho^{(o)}}$$

$$\omega_c = \frac{\Gamma^{(o)}}{\frac{3}{2}\rho_o T^{(o)}}.$$

This gives us a fourth order equation for  $\omega(k)$  of the form

$$k^{4} \left( 1 - \frac{i\omega v'}{c_{t}^{2}} \right) + k^{2} \left( \frac{-\omega^{2}}{c_{t}^{2}} + \frac{\omega_{c}}{\chi} \left( 1 - \frac{-i\omega v'}{c_{t}^{2}} \right) \right)$$
$$\frac{-i\omega}{\chi} \left( 1 - \frac{i\omega v'}{c_{t}^{2}} \right) \frac{-i\omega c_{\rho}^{2}}{\frac{3}{2}\rho^{(o)}\chi} + \frac{\omega^{2}}{\chi c_{t}^{2}} (i\omega - \omega_{c}) = 0.$$

The remainder of this section will be devoted to examining the consequences of the above dispersion relation.

Before proceeding it is worthwhile to digress and consider the same problem for normal fluid. There,  $\omega_{\rm c}=0$  since there is no dissipation. For gases the kinematic viscosity  $\nu'$  is negligible compared to the thermal diffusivity. If we define a frequency  $\omega_{\chi}=c_t^2/\chi$  we can distinguish two limits

(a) 
$$\omega \ll \omega_{\chi}$$
:

$$c_t^2 k^2 \quad \left(1 + \frac{c_\rho^2}{\frac{3}{2}\rho(o)}\right) = \omega^2$$
$$= c_s^2 k^2$$

where  $c_s$  is the adiabatic sound speed. There is also an absorption coefficient where

$$k = \frac{\omega}{c_s} + ia\omega^2, \qquad a \sim \chi$$

(b) 
$$\omega \gg \omega_{\rm x}!$$

Now we get approximately isothermal propagation since the temperature field is frozen on the time side of the density fluctuation. Now

$$k = \frac{\omega}{c_t} + ia' \quad a' \sim \frac{1}{\chi}.$$

Of course,  $\nu'$  is not exactly zero and eventually becomes important. If  $\omega$  is much bigger than  $w'_{\nu}=c_t^2/\nu'$ , we then get a balance of the form

$$\frac{-i\omega k^4}{\omega_{\nu'}} = \frac{k^2\omega^2}{c_i^2} \to k = \sqrt{\frac{i\omega}{\nu'}}.$$

For air, this occurs at frequencies of  $10^9$  Hz; for water at  $10^{12}$  Hz. Hence these viscous regimes are not of much practical importance. There is of course also a second mode at small frequency

$$k = \sqrt{\frac{i\omega}{\chi}}$$

which corresponds to thermal diffusion, with no velocity or density perturbation.

We now return to the granular fluid. The major difference is that temperature fluctuations are damped even at low frequency. Assuming that  $\omega$  is smaller than all other frequency  $(\omega_c, \omega_{\chi}, \text{ and } \omega_{\nu'} = c_t^2/\nu')$  we obtain

$$k = \frac{\omega}{c_t} + i\omega^2 a \quad a \sim 1/\omega_c.$$

That is, the propagation is isothermal! At high frequencies, we again have purely damped motion with two possible modes

$$k = \sqrt{\frac{i\omega}{\chi}}$$
 or  $k = \sqrt{\frac{i\omega}{\nu'}}$ .

Again, there is also a second mode at small frequency which is purely damped, as expected from the discussion above.

Why are these modes interesting? First of all, it offers a completely new methodology for testing the continuum theory of granular flow. It is certainly possible to set up a shear flow and measure all the relevant material properties (It is also possible to calculate them within the context of a kinetic theory which starts from particle collisions, but this is not likely to yield much quantitatively valid information). Once all these parameters are known, we would have a prediction of the sound speed and the relationship between density and temperature fluctuations. Via exciting these modes with, say, an oscillatory variation of the driving plate, one could test this entire framework.

There is a second reason why sound modes are vital. To see this, recall that in a granular flow all velocities are ultimately related to the shear rate imposed on the flow. For example, in Section 3 we saw that the typical fluctuation velocity  $v_T \sim T^{1/2}$  is proportional to  $\dot{\gamma}\sigma$  where  $\sigma$  is the particle size. Let us therefore consider the Mach number of a typical flow

$$M = v/c_t$$
.

Now  $v \sim \dot{\gamma}L$  where L is the system depth and  $c_t \sim \sqrt{\frac{\partial p}{\partial \rho}} \sim T^{1/2} \sim \dot{\gamma}\sigma$ . Hence the ratio  $M \sim L/\sigma$  times some complicated function of density. Since L must be at least tens of particle sizes for a macroscopic theory to make any sense, we have the simple result that many typical flows will be <u>supersonic</u>.

The above statement again has many interesting consequences for testing the validity of continuum theories. We would predict for example that placing an obstacle in the flow would cause the formation of shock-like fronts in the density. It should be noted, however, that the highly dissipative nature of granular fluids (i.e. large viscosity and temperature fluctuation dumping) will tend to significantly broaden such fronts. Also, any nascent instability in the steady flow would couple to compressibility in a highly nontrivial manner. Such effects form the subject matter of the next section.

Although most of the results in this work have dealt with the granular flow system, we would like to remark on density fluctuations in a viscous suspension. As mentioned at the end of Section 2, one proposed model for viscous suspensions would be a similar set of hydrodynamic equations with the replacement

$$ho o rac{\mu}{\sigma\sqrt{T}}$$
.

Doing this makes the pressure independent of the particle density. This removes the basic driving force for wave phenomena and one can show that all modes are damped. The two modes respectively are temperature which is just damped and density which is diffusive, i.e.  $\omega \sim ik^2$ . This is quite reasonable since the only sound waves expected in the system rely on the compressibility of the ambient fluid to transmit fluctuations. This is not irrelevant in lubrication force dominated regimes.

### 6 INSTABILITIES IN GRANULAR FLOW

In this section, we consider possible instabilities which may transform steady granular flow patterns into more complex spatial and temporal structures. Again, a major motivation is to provide a variety of qualitative tests of the idea of treating solid-liquid systems via a one phase continuum theory. In fact, there is some evidence of anomalous fluctuations associated with "flow disorder" in experiments of Savage and Sayed as well as the hopper flow of Baxter et al. In the hopper flow, these fluctuations are probably connected with observed density waves which propagate through the system.

Let us focus on a Taylor-Coutte system as an example of a granular flow instability. First, let us recall the classical case of an incompressible flow. Our base flow is purely azimuthal

$$\vec{V}^{(o)} = v(r)\hat{\Theta}.$$

Assuming a small perturbation  $\hat{v}_r, \hat{v}_{\Theta}, \hat{\rho}$ , we have

$$\frac{\rho^{(o)}\partial\hat{v}_{r}}{\partial t} = 2\rho^{(o)}\Omega(r)\hat{v}_{\theta} - \frac{\partial\hat{p}}{\partial r} 
\frac{\rho^{(o)}\partial\hat{v}_{z}}{\partial t} = -\frac{\partial\hat{p}}{\partial z} 
\frac{\rho^{(o)}\partial\hat{v}_{\Theta}}{\partial t} = \frac{-v_{r}}{r}\rho^{(o)}\frac{\partial}{\partial r}(r^{3}\Omega(r)).$$

Now the vorticity of the original profile  $\Omega(r) = v_{\Theta}(r)/r$  is arbitrary at zero viscosity. If we include viscosity in the base solution while still neglecting it for the perturbative analysis, we should take

$$\Omega = \Omega_o + \frac{\Omega_1}{r^2}$$

since the original momentum equation takes the form

$$0 = \mu \left( \frac{\partial^2}{\partial r^2} + \frac{1}{r} \frac{\partial}{\partial r} - \frac{1}{r^2} \right) V_{\Theta}(r)$$
$$= r \mu \left( \frac{\partial^2}{\partial r^2} + \frac{3}{r} \frac{\partial}{\partial r} \right) \Omega(r).$$

Returning to the stability calculation, incompressibility demands

$$k_z \hat{V}_z = -k_r \hat{v}_r.$$

We can eliminate  $\frac{\partial \hat{p}}{\partial r}$  by recognizing that

$$\frac{1}{\rho^{(o)}}\frac{\partial \hat{p}}{\partial r} = \frac{1}{\rho^{(o)}}\frac{k_r}{k_z}\frac{\partial \hat{p}}{\partial z} = \frac{-k_r}{k_z}\frac{\partial v_z}{\partial t} = \left(\frac{k_r}{k_z}\right)^2\frac{\partial v_r}{\partial t}.$$

Substituting this and also the equation  $v_{\Theta}$  into the equation for  $\partial v_{\tau}/\partial t$ , we get the dispersion relation

$$i\omega = \frac{2\Omega i}{\omega} \frac{\partial}{\partial r} (r^2 \Omega) + i\omega \left(\frac{k_r}{k_z}\right)^2$$

or

$$\omega^{2} = \frac{k_{z}^{2}\Phi}{k_{r}^{2} + k_{z}^{2}}$$
$$\Phi = \frac{2\Omega}{r}\frac{\partial}{\partial r}(r^{2}\Omega).$$

The instability criteria thus reduces to the well-known Rayleigh criterion  $\Phi < 0$  for all r. This can be employed to show that as Taylor-Couette cell with counter-rotating cylinders is always unstable whereas stability persists in the co-rotating case until the rotation ratio exceeds a critical value.

We now would like to understand what happens if one reconsiders the above analysis in the case of a granular fluid. The first point is that there may be significant stratification due to the centrifugal force. Specifically, momentum balance in the  $\hat{r}$  direction requires

$$\frac{dp}{dr} = \frac{\rho v^2}{r}$$

and using  $p \sim \rho T$ 

$$\rho T = \rho_o T_o \exp \int_{r_o}^{r} \frac{r' \Omega^2(r')}{p_o T(r')} dr'$$

where  $V(r)=r\Omega(r)$ . The corresponding vorticity profile now obeys the modified equation

$$0 = \mu \left( \frac{\partial^2}{\partial r^2} + \frac{3}{r} \frac{\partial}{\partial r} \right) \Omega + \frac{\partial \mu}{\partial r} \frac{\partial \Omega}{\partial r}$$

whose solution, using  $\mu = \mu_o \rho T^{1/2}$ , is

$$\Omega = \Omega_o + \Omega_1 \int_{r_o}^r \frac{1}{r'^3} \rho T^{1/2}(r') dr'.$$

The system of equations for  $\rho T$  and  $\Omega$  is now closed by writing down the energy equation. Clearly, this is quite complicated. However, our main point is that there may be a strongly inhomogeneous distribution of density and temperature in anything other than the thin gap limit.

We now turn to a study of the stability of this equilibrium state. We have the set of equations

$$\rho^{(o)} \frac{\partial \hat{v}_{\Theta}}{\partial t} = \frac{\hat{v}_{r}}{r} \frac{\partial}{\partial r} (r^{2} \Omega) \rho^{o}$$

$$\rho^{(o)} \frac{\partial \hat{v}_{z}}{\partial t} = -\frac{\partial}{\partial z} \left( \frac{\gamma^{(o)}}{\rho^{(o)}} \hat{\rho} + \frac{p^{(o)}}{T^{(o)}} \hat{\rho} + \frac{p^{(o)}}{T^{(o)}} \hat{T} \right)$$

$$\rho^{(o)} \left( \frac{\partial \hat{v}_{r}}{\partial t} - 2\Omega \hat{v}_{\theta} \right) - \frac{\hat{\rho} v_{\theta}^{2}}{r} = \frac{-\partial}{\partial r} \left( \frac{p^{(o)}}{\rho^{(o)}} \hat{\rho} + \frac{P^{(o)}}{T^{(o)}} \hat{T} \right)$$

for momentum conservation;

$$\frac{\partial \hat{\rho}}{\partial t} + \hat{v}_r \frac{\partial \rho^{(o)}}{\partial r} = -\rho^{(o)} \vec{\nabla} \cdot \hat{v}$$

for density variations, and the energy equation, in the limit  $\omega \gg w_c$  (and all other dissipative frequencies) has the form

$$\frac{\partial \hat{T}}{\partial t} + \hat{v}_r \frac{\partial T^{(o)}}{\partial r} = -\frac{2}{3} \frac{p^{(o)}}{\rho^{(o)}} \vec{\nabla} \cdot \hat{v}.$$

The key difference between these equations and the ones from the normal fluid is the presence of density fluctuations which then couple to temperature fluctuations.

We will, for simplicity, deal with the highly supersonic limit

$$\omega \gg kc_t$$
.

In this limit, we can drop the  $\vec{\nabla} \cdot \hat{V}$  term in the temperature and density equation, since convection is much more rapid than transmission by acoustic waves. So

$$\hat{V}_{\theta} = \frac{\hat{v}_{\tau}}{i\omega r} \frac{\partial}{\partial r} (r^{2}\Omega) 
\hat{V}_{\tau} = \frac{-1}{i\omega} \left( 2\Omega \hat{V}_{\theta} + \frac{\hat{\rho}V_{\theta}^{2}}{V \rho^{(o)}} \right) + O\left( \frac{c_{t}k}{\omega} \right).$$

From the density equation

$$\hat{\rho} = \frac{\hat{V}_r}{i\omega} \frac{\partial \rho^{(o)}}{\partial r}$$

substituting the  $\hat{V}_{ heta}$  equation to the  $\hat{V}_{ au}$  one, we find the dispersion relation

$$\omega^2 = \Phi + \frac{V_\theta^2}{\rho^{(o)}r} \frac{\partial \rho^{(o)}}{\partial r} + 0 \left(\frac{c_t k}{\omega}\right).$$

Comparing this formula to the preceding one, we see the presence of a new term related to the stratification  $\frac{1}{\rho(o)} \frac{\partial \rho(o)}{\partial r}$ . If the material is more dense at larger radius (certainly the expected effect of the centrifugal term), this will tend to stabilize the system, essentially via a Rayleigh-Taylor density interchange. The upshot is that we observe an interesting coupling between angular momentum and density stratification, which will change the stability criterion as well as the character of the unstable mode.

The above analysis suggests that it would be very interesting to systematically investigate all the "typical" fluid instabilities for granular liquids. For the completely supersonic resinc  $\omega \gg kc_t$  (as well all dissipative frequencies), this amounts to including compressibility. For smaller  $\omega$  (and hence for the onset of all non-oscillatory instabilities) the strong damping of temperature fluctuations will be important (and presumably ensure that growing modes are mostly isothermal), as will the coupling to density fluctuations. Again, these hydrodynamic tests of the granular flow concept are much more interesting than mere viscometric tests which have already been performed to date.

## 7 CONCLUSIONS

In this report, we have explored the single-phase continuum model proposed by Jenkins and Savage (1982) to describe granular flow. Many of our results can be extended to make predictions for dense suspensions, which can be described using a similar theoretical framework. The goal has been to develop clear, qualitative predictions that appear to be amenable to experimental verification. In particular, our analysis suggests that an increased battery of hydrodynamic tests on granular (and dense suspension) systems could be developed that would be more effective in sorting out valid model approaches compared with proceeding directly to expensive, quantitative tests. We would strongly oppose large-scale simulations or quantitative tests of this or any other model until the model passes these types of qualitative tests and its assumptions have been validated.

The key results from our analysis of granular flow based on the singlephase continuum model include the following.

- We have predicted the flow profiles for simple boundary conditions, such as plane Couette flow and channel flow. From these studies, macroscopic and microscopic criteria for the model's validity have been developed. For the potentially valid range of concentration and velocity, pressure and shear stress should scale quadratically with shear rate, and there should be a near-balance between viscous heating and collisional dissipation on microscopic scales.
- We have argued that the model predicts segregation effects when there are two (or more) particle sizes considered. In shear flow, large particles should rise in a gravitational field compared to small grains, perhaps producing double-diffusive fingering in some limits.

- We have derived the acoustic dispersion relations and shown that they predict granular flow to be supersonic. This result can be verified by measuring the sound speed in shear flows. Also, the flow past bodies in granular shear flows should reveal disturbances only past the leading edge of the body and broadened shock fronts characteristic of dissipative flow.
- We point out that the analysis of flow instabilities is complicated by the finite compressibility of the solid-fluid mixture. For example, the finite compressibility leads to the prediction of density interchange (Rayleigh-Taylor instabilities) in addition the usual angular momentum interchange in standard (cylindrical) Couette flow.

We believe that these predictions suggest a series of experiments that can form the basis of an exciting, insightful, and (hopefully) inexpensive program of research on solid-fluid flow. Because of their qualitative nature, these tests should provide an empirical verification of theoretical models that is less sensitive to the details of the system. In the Appendix, we outline existing and potential approaches for imaging multiphase flow, which would be a key component in developing the experimental program.

# A IMAGING SOLID-GAS AND SOLID-LIQUID FLOWS

In Section 1, we commented on the need for an expanded range of qualitative hydrodynamic tests of theories before considering expensive, large-scale computer simulations. For example, several different types of experiments were suggested in the discussion of the single-phase continuum model of solid-fluid flow. A common need in all of these qualitative tests is detailed information about particle-fluid positions and velocities.

Imaging techniques of various types have been developed by many researchers to gather this information. Some of these approaches are restricted to special, ideal test systems; others can be applied in the real plant environment, as well. However, as we discuss below, none of these techniques is sufficiently powerful to provide a general solution to the imaging problem. Thus, an important component of experimental research in this area should be the improvement of imaging techniques.

Because this issue is so closely tied to the development of theory, we thought it might be useful to comment on present and projected imaging methods. Below, we briefly discuss imaging techniques for both solid-liquid and solid-gas flows. The flows important for applications often have a relatively rapid time development. An ideal imaging system would provide two-or three-dimensional images of the different phases in the flow with good time resolution and with little or no perturbation of the flow. One must also bear in mind that the flow often creates a hostile environment for sensors, for example, by sand-blasting. As we will find below, these goals are difficult to meet.

# A.1 Non-Invasive Techniques

#### Electrical

Capacitance probe: In this technique, used by Louge and collaborators at Cornell, a capacitive probe is located along the wall of a pipe containing a particulate suspension. The probe is sensitive to changes in dielectric constant between the fluid and solid. With care, excellent sensitivity can be achieved using commercially available electronics. This technique can be readily extended to arrays of capacitive probes to provide some spanish information.

Present geometry by Louge et al. needs to be improved for better control of fields. ADVANTAGES: fast; sensitive; rugged probe; relative cheap. DIS-ADVANTAGES: local probe only senses flow near surface; pickup area not sharply defined.

Inductive pickup: A pickup coil is wound around the outside of the pipe. For particular flows, the particles often acquire an electrostatic charge, which produces a pulse in the pickup coil when the particle pass through. One can also imagine charging particles with an electrical discharge. Multiple pickups could be used along the pipe. ADVANTAGES: fast, cheap; rugged. DISADVANTAGES: shielded by metal pipes; pickup has spatial resolution only along the pipe; works only for charged particle such as sand grains in gases; details of charging difficult to control and may influence flow.

#### Acoustic

Sound-passive microphones: Conventional contact microphones are attached along the outside of the pipe. Spectrum analysis may provide some useful information about the flow. ADVANTAGES: fast; cheap; portable;

could be installed along pipelines in plants as an online diagnostic. DISAD-VANTAGES: nonlocal pickup; hard to analyze quantitatively.

Pressure probes: Conventional pickups are used to measure the pressure in the flow. For fluidized beds, this is a good measure of the average particulate content. ADVANTAGES: reliable; cheap; simple interpretation. DISADVANTAGES: poor spatial resolution; only work near pipe surface.

## Optical

Optical imaging with tracer particles: In this technique, visible tracer particles are added to a multiphase flow which is made transparent by using transparent liquid and particles with matched indices of refraction. If the tracers have properties similar to particles, then one images the particle flow; if they are flow visualizers such as "fish scales," then one images the fluid. These techniques and variants are used for the study of ideal systems in the laboratory (e.g., J. R. Kadambi, Case Western Reserve). ADVANTAGES: visual; 3D, fast; easy to interpret; uses conventional photographic and computer techniques; relatively low cost. DISADVANTAGES: limited to ideal systems only.

Optical imaging with laser induced fluorescence or color change: This technique also requires transparent multiphase flow, and hence is limited to ideal systems. As in the work of R. Falco (Michigan State), a high power laser is used to induce a short-lived fluorescence or color change in either the particles or the liquid of a multiphase flow in a well-defined pattern, such as a grid. Thus, the flow is tagged at one instant with a pattern. The distortion of this pattern in time allows one to derive the local motion of the particles or fluid, including the local vorticity. We strongly recommend that the Falco and Kadambi (previous technique) groups be in close contact to share technology and speed development of the optimal technique. ADVANTAGES: visual; 3D; fast; easy to interpret; uses conventional photographic techniques;

computer image processing permits mapping of local velocity and vorticity profiles. DISADVANTAGES: precise index match limits technique to ideal systems; relatively high cost of laser and computer image processor.

## Medical Techniques

In developing the ideal imaging technique for solid-fluid flow, one is faced with a problem already encountered in medicine, i.e., how to image solids suspended in water using non-invasive techniques. An enormous effort has been made to develop these techniques in the medical area, with many notable successes: sophisticated x-ray imaging, x-ray tomography, ultrasonic and magnetic resonance imaging. The equipment required is often very expensive (over 1M machine), but is readily available in many medical centers located throughout the country for use in cooperative research or simply for an hourly fee. For example, Behringer cite BEH has collaborated with the Medical School at Duke University to make time-resolved x-ray images of flowing sand. The use of these facilities can be a sensible and cost-effective solution for those experiments which can be transported.

X-ray imaging: Standard x-ray cameras can be used to image multiphase flows. Digital image subtraction can be used to detect changes in flow, as in the research of Behringer (Duke). ADVANTAGES: standard technique easily accessible in hospitals; good time resolution for short bursts of images. DISADVANTAGES: 2D image; expensive if not in hospital; low contrast if used for liquid-gas mixtures.

X-ray tomography: Conventional CAT scanner. ADVANTAGES: 3D image; available at many medical centers; excellent detail. DISADVANTAGES: too slow for many applications; prohibitively expensive outside of hospital.

NMR imaging: Conventional magnetic resonance imager. ADVANTAGES: 3D image; available at many medical centers; excellent detail and contrast. DISADVANTAGES: very slow; prohibitively expensive outside of hospital.

Ultrasonic imaging: Conventional medical ultrasonic imaging instrumentation. The application to multiphase flows is questionable but worth investigation. Its success will depend upon the acoustic background created by the flow at ultrasonic frequencies and by clutter created by multiple scattered returns. ADVANTAGES: available at hospitals; portable apparatus; moderate expense. DISADVANTAGES: less resolution; slow; high background noise level and clutter from flow; requires liquid medium.

## A.2 Invasive Techniques

Capacitance probes: The technique is similar to the non-invasive counterpart above, except that the probe is positioned in the flow. Arrays of probes can also be used with greater perturbation of the flow. If the prediction that the flow is supersonic is correct (Section 4), then probe only disturbs flow past the measuring point. ADVANTAGES: as above; mapping of concentration profiles possible; probes can be small and rugged. DISADVANTAGES: single point measurements; pickup area not sharply defined; perturbs flow.

Velocimeter probes: Laser induced fluorescence can be used to tag a single particle at a given instant. The motion of the particle is then tracked using optical probes (for example, an array of fiber-optic pickups or photodiodes), and the timing of its passage used to determine the magnitude and direction of its velocity. The laser light can be brought to the end of a small probe using fiber-optics. ADVANTAGES: mapping of velocity profiles; fast; potentially small and rugged. DISADVANTAGES: single point measurement; perturbs flow.

Sampling probes: Here a hollow probe is simply used to collect a sample of the particles at a given position. ADVANTAGES: mapping of particle characteristics vs. position to test for segregation, etc. DISADVANTAGES: slow; time averaged; perturbs flow.

#### REFERENCES

- 1. H. Abarbanel, H. Levine, and P. Steinhardt, "DOE Sponsored Research in Multiphase Flow," JSR-88-330, March 1989.
- D. J. Jeffrey and A. Acrivos, AIChE J. 22, 417 (1976). D. Leighton and A. Acrivos, J. Fluid Mech. 177, 109 (1987); 181, 415 (1987); Chem. Eng. Sci 41, 1377 (1986).
- 3. J. F. Brady and G. Bossis, J. Fluid Mech. 44, 1 (1970).
- 4. R. A. Bagnold, Proc. Roy. S. Lond A 225, 49 (1954); A295, 295 (1966).
- 5. S. B. Savage and M. Sayed, J. Fluid Mech 142, 391 (1984).
- 6. O. Walton and R. L. Braun, Acta Mech. 63, 73 (1986).
- 7. R. Jackson, "Hydrodynamic Stability of Fluid-Particle Systems" in Fluidization, ed. by J. F. Davidson, R. Clift and D. Harrison (Academic Press, 1988), p. 47; D. Gidaspow, Appl. Mech. Rev. 39, 1 (1986).
- 8. J. T. Jenkins and S. B. Savage, J. Fluid Mech. 130 187 (1983).
- 9. J. T. Jenkins and D. F. McTigue, to appear in *Proc. IMA Workshop on Multiphase Flow*, ed. by D. Joseph and D. Schaffer, (Springer-Verlag, New York).
- 10. P. K. Haff, J. Fluid Mech. 134, 401 (1983).
- G. W. Baxter, R. Behringer, T. Fagert, G. A. Johnson, Phys. Rev. Lett., 62, 282S (1989).
- 12. C. Campbell, Ann. Rev. Fluid Mech. 22, 57 (1990).
- 13. P. C. Johnson and R. Jackson, J. Fluid Mech. 176, 67 (1987).
- 14. D. M. Hanes, J. T. Jenkins and M. W. Richman, J. of Applied Mech. 55 969 (1985).
- 15. S. B. Savage and C. K. Lun, J. Fluid Mech. 189, 311 (1988).
- R. H. Weiland, Y. P. Fessas and B. V. Ramarao, J. Fluid Mech 142, 383 (1984).
- 17. D. M. Hanes and D. I. Inman, J. Geophys. Res., 90, 3670 (1985).
- 18. H. M. Jaeger, C. H. Liu and S. R. Nagel, Phys. Rev. Lett 62, 40 (1989).
- 19. D. G. Schaeffer, J. Diff. Eq 66, 19 (1987).

Director Ames Laboratory [2] Iowa State University Ames, IA 50011

Mr John M Bachkosky Deputy DDR&E The Pentagon Room 3E114 Washington, DC 20301

Dr Joseph Ball Central Intelligence Agency Washington, DC 20505

Dr Arthur E Bisson DASWD (OASN/RD&A) The Pentagon Room 5C675 Washington, DC 20350-1000

Dr Albert Brandenstein Chief Scientist Office of Natl Drug Control Policy Executive Office of the President Washington, DC 20500

Mr Edward Brown Assistant Director Nuclear Monitoring Research Office DARPA 3701 North Fairfax Drive Arlington, VA 22203 Dr Herbert L Buchanan III Director DARPA/DSO 3701 North Fairfax Drive Arlington, VA 22203

Dr Curtis G Callan Jr Physics Department PO Box 708 Princeton University Princeton, NJ 08544

Dr Ferdinand N Cirillo Jr Central Intelligence Agency Washington, DC 20505

Brig Gen Stephen P Condon Deputy Assistant Secretary Management Policy & Program Integration The Pentagon Room 4E969 Washington, DC 20330-1000

Ambassador Henry F Cooper Director/SDIO-D Room 1E1081 The Pentagon Washington, DC 20301-7100

DARPA RMO/Library 3701 North Fairfax Drive Arlington, VA 22209-2308

Mr John Darrah Senior Scientist and Technical Advisor HQAF SPACOM/CN Peterson AFB, CO 80914-5001

Dr Patrick H Diamond
Department of Physics
Mayer Hall/B-019/Room 4110
University of California/San Diego
La Jolla, CA 92093

Col Doc Dougherty DARPA/DIRO 3701 North Fairfax Drive Arlington, VA 22203

DTIC [2]
Defense Technical Information Center
Cameron Station
Alexandria, VA 22314

Dr James M Ekmann
US Department of Energy
Pittsburgh Energy Technology Center
PO Box 10940
Cochrans Mill Road
Pittsburgh, PA 15236

Mr John N Entzminger Chief, Advance Technology DARPA/ASTO 3701 North Fairfax Drive Arlington, VA 22203 CAPT Kirk Evans
Director Undersea Warfare
Space & Naval Warfare Sys Cmd
Code PD-80
Department of the Navy
Washington, DC 20363-5100

Dr Robert Falco
Dept of Mechanical Engineering
Michigan State University
East Lansing, MI 48824

Mr Frank M Ferrell [2] FE-14/GTN US Department of Energy Washington, DC 20585

Mr F Don Freeburn US Department of Energy Code ER-33 Mail Stop G-236 Washington, DC 20585

Dr Fred M Glaser [10]
Office of Technical Coordination
U S Department of Energy
FE-14/GTN
Washington, DC 20545

Dr S William Gouse Sr Vice President and General Manager The MITRE Corporation Mail Stop Z605 7525 Colshire Drive McLean, VA 22102

LTGEN Robert D Hammond CMDR & Program Executive Officer US Army/CSSD-ZA Strategic Defense Command PO Box 15280 Arlington, VA 22215-0150

Mr Thomas H Handel Office of Naval Intelligence The Pentagon Room 5D660 Washington, DC 20350-2000

Maj Gen Donald G Hard Director of Space and SDI Programs Code SAF/AQS The Pentagon Washington, DC 20330-1000

Dr Jeffrey Alan Harvey Enrico Fermi Institute 5640 Ellis Avenue Chicago, IL 60637-1433

Dr Robert G Henderson Director JASON Program Office The MITRE Corporation 7525 Colshire Drive Z561 McLean, VA 22102

Dr Barry Horowitz President and Chief Executive Officer The MITRE Corporation Burlington Road Bedford, MA 01730 Dr William E Howard III [2]
Director For Space
and Strategic Technology
Office/Assistant Secretary of the Army
The Pentagon Room 3E474
Washington, DC 20310-0103

Dr Gerald J Iafrate US Army Research Office PO Box 12211 4300 South Miami Boulevard Research Triangle Park, NC 27709-2211

Technical Information Center [2] US Department of Energy PO Box 62 Oak Ridge, TN 37830

JASON Library [5] The MITRE Corporation Mail Stop W002 7525 Colshire Drive McLean, VA 22102

Dr George Jordy [25] Director for Program Analysis US Department of Energy MS ER30 Germantown OER Washington, DC 20585

Dr O'Dean P Judd Los Alamos National Lab Mail Stop A-110 Los Alamos, NM 87545

Dr George Klinzing University of Pittsburgh 323 Benedum Hall Pittsburgh, PA 15261

Dr Ted Knowlton Institute of Gas Technology 4201 West 36th Street Chicago, IL 60632

Dr Herbert Levine
Department of Physics
Mayer Hall/B019
University of California/San Diego
La Jolla, CA 92093

Technical Librarian [2] Argonne National Laboratory 9700 South Cass Avenue Chicago, IL 60439

Research Librarian [2] Brookhaven National Laboratory Upton, NY 11973

Technical Librarian [2] Los Alamos National Laboratory PO Box 1663 Los Alamos, NM 87545 Technical Librarian [2] Pacific Northwest Laboratory PO Box 999 Battelle Boulevard Richland, WA 99352

Technical Librarian [2] Sandia National Laboratories PO Box 5800 Albuquerque, NM 87185

Technical Librarian [2] Sandia National Laboratories PO Box 969 Livermore, CA 94550

Technical Librarian [2] Lawrence Berkeley Laboratory One Cyclotron Road Berkeley, CA 94720

Technical Librarian [2] Lawrence Livermore Nat'l Lab PO Box 808 Livermore, CA 94550

Technical Librarian [2]
Oak Ridge National Laboratory
Box X
Oak Ridge, TN 37831

Chief Library Branch [2] AD-234.2 FORS US Department of Energy Washington, DC 20585

Professor Michael Louge Department of Mechanical Engineering Upson Hall Cornell University Ithaca, NY 14853

Mr Robert Madden [2] Department of Defense National Security Agency Attn R-9 (Mr Madden) Ft George G Meade, MD 20755-6000

Dr Arthur F Manfredi Jr [10] OSWR Central Intelligence Agency Washington, DC 20505

Dr Oscar P Manley Office of Basic Energy Research Dept of Energy Code ER-15/GTN Washington, DC 20545

Mr Joe Martin
Director
OUSD(A)/TWP/NW&M
Room 3D1048
The Pentagon
Washington, DC 20301

Dr Mehrada Massoudi US Department of Energy Pittsburgh Energy Technology Center PO Box 10940 Cochrans Mill Road Pittsburgh, PA 15236

Mr Ronald Murphy DARPA/ASTO 3701 North Fairfax Drive Arlington, VA 22203-1714

Dr Julian C Nall Institute for Defense Analyses 1801 North Beauregard Street Alexandria, VA 22311

Dr Gordon C Oehler Central Intelligence Agency Washington, DC 20505

Oak Ridge Operations Office Procurement and Contracts Division US Department of Energy (DOE IA No DE-AI05-90ER30174) PO Box 2001 Oak Ridge, TN 37831-8757

Dr Peter G Pappas Chief Scientist US Army Strategic Defense Command PO Box 15280 Arlington, VA 22215-0280

Dr Steven Passmann Sandia Nat'l Labs Livermore PO Box 969 Livermore, CA 94551-0969

Dr William Peters US Department of Energy Pittsburgh Energy Technology Center PO Box 10940 Cochrans Mill Road Pittsburgh, PA 15236

Dr Bruce Pierce USD(A)/D S Room 3D136 The Pentagon Washington, DC 20301-3090

Mr John Rausch [2] Division Head 06 Department NAVOPINTCEN 4301 Suitland Road Washington, DC 20390

Records Resources
The MITRE Corporation
Mailstop W115
7525 Colshire Drive
McLean, VA 22102

Dr Fred E Saalfeld Director Office of Naval Research 800 North Quincy Street Arlington, VA 22217-5000 Dr John Schuster
Technical Director of Submarine
and SSBN Security Program
Department of the Navy OP-02T
The Pentagon Room 4D534
Washington, DC 20350-2000

Dr Barbara Seiders Chief of Research Office of Chief Science Advisor Arms Control & Disarmament Agency 320 21st Street NW Washington, DC 20451

Dr Philip A Selwyn [2] Director Office of Naval Technology Room 907 800 North Quincy Street Arlington, VA 22217-5000

Dr Paul Joseph Steinhardt David Rittenhouse Laboratory Department of Physics 33rd & Walnut Streets University of Pennsylvania Philadelphia, PA 19104-6396

Superintendent CODE 1424 Attn Documents Librarian Naval Postgraduate School Monterey, CA 93943

Dr George W Ullrich [3] Deputy Director Defense Nuclear Agency 6801 Telegraph Road Alexandria, VA 22310

Ms Michelle Van Cleave Asst Dir/National Security Affairs Office/Science and Technology Policy New Executive Office Building 17th and Pennsylvania Avenue Washington, DC 20506

Mr Richard Vitali Director of Corporate Laboratory US Army I aboratory Command 2800 Powder Mill Road Adelphi, MD 20783-1145

Dr Otis R Walton Lawrence Livermore Nat'l Lab L-207 PO Box 808 Livermore, CA 94551

Dr Robert M Westervelt Division of Applied Sciences Harvard University Cambridge, MA 02138

Dr Edward C Whitman
Dep Assistant Secretary of the Navy
C3I Electronic Warfare & Space
Department of the Navy
The Pentagon 4D745
Washington, DC 20350-5000

Mr Donald J. Yockey U/Secretary of Defense For Acquisition The Pentagon Room 3E933 Washington, DC 20301-3000 Dr Linda Zall Central Intelligence Agency Washington, DC 20505

Mr Charles A Zraket Trustee The MITRE Corporation Mail Stop A130 Burlington Road Bedford, MA 01730